Bernoulli **8**(1), 2002, 53–80

Inverse method of images

VIOLET S.F. LO[1], GARETH O. ROBERTS[2] and HENRY E. DANIELS

[1]*Deutsche Bank AG, 1 Great Winchester Street, London EC2N 2DB, UK.*
[2]*Department of Mathematics and Statistics, Lancaster University, Lancaster, LA1 4YF, UK.*
E-mail: g.o.roberts@lancaster.ac.uk

We consider the problem of approximating the density of the time at which a Brownian path first crosses a curved boundary in cases where the exact density is not known or is difficult to compute. Approximation methods which involve the use of images will be proposed. These methods can be used not only for one-sided boundaries but also for the case of two-sided boundaries; and not only for concave boundaries but also for convex boundaries. The square root boundary and parabolic boundary provide examples for numerical comparisons of the approximation methods.

Keywords: boundary crossing probabilities; Brownian motion; method of images

1. Introduction

The distribution of the first exit time of a one-dimensional diffusion process from some given boundary is of major importance in sequential analysis, optimal stopping problems and other contexts where the probability that a random walk crosses a general boundary for the first time is to be evaluated. This paper is concerned with estimating the density or distribution of the time at which a Brownian motion first exits a curved boundary in cases where the exact solution is not known or is difficult to compute. We propose approximation methods which apply to any one-sided or two-sided curved boundary.

Suppose that X is a one-dimensional diffusion process and ψ is a given one-sided curved boundary with $X_0 < \psi(0)$. Then the first hitting time of X with respect to ψ from below, τ_ψ, is

$$\tau_\psi = \inf_{t>0} \{t : X_t \geqslant \psi(t)\}.$$

If, alternatively, $\psi = (\psi_+, \psi_-)$ is a two-sided boundary with $\psi_-(0) < X_0 < \psi_+(0)$ and $\psi_-(t) \leqslant \psi_+(t)$ for $t > 0$, then the first exit time of X from ψ is given by

$$\tau_{\psi_\pm} \equiv \tau_{\psi_+} \wedge \tau_{\psi_-} = \inf_{t>0} \{t : X_t \geqslant \psi_+(t) \text{ or } X_t \leqslant \psi_-(t)\}.$$

In the case where X is a Brownian motion process and the boundary ψ is linear, $\psi(t) = \alpha + \beta t$, the first exit-time density of X with respect to ψ has a simple closed form known as the *Bachelier–Lévy formula*,

$$P(\tau \in \mathrm{d}t) = \frac{\alpha}{t^{3/2}} \phi\left(\frac{\alpha + \beta t}{\sqrt{t}}\right) \mathrm{d}t,$$

where ϕ is the standard normal density function. The corresponding probability distribution is given by

$$P(\tau \leqslant t) = 1 - \Phi\left(\frac{\alpha + \beta t}{\sqrt{t}}\right) + \mathrm{e}^{-2\alpha\beta}\Phi\left(\frac{\beta t - \alpha}{\sqrt{t}}\right).$$

However, there are few exact solutions available for those cases where the boundary is non-linear, and a good approximation which produces solutions in compact and explicit form with simple calculations is desirable.

There are several approximation methods available for estimating the first hitting-time density of a Brownian motion process with respect to a general boundary, namely, the tangent approximation (Strassen 1967; Lerche 1986), series expansion methods (see, for example, Durbin 1992), and the hazard rate tangent approximation (Roberts and Shortland 1995). Most of these methods can be thought of as special cases of the so-called method of images (Daniels 1982; Lerche 1986), although general use of this method is restricted by the need to invert the solution of a partial differential equation as a function of the boundary condition. Daniels (1996) discussed two developments of the method of images. The first led to an improvement of the tangent approximation. The second, by discretizing an integral equation, allowed the calculation of an accurate approximation for general boundaries. The present paper is essentially a sequel to and development of the material in Daniels (1996). We exploit the use of images for approximating the first hitting-time density of a Brownian motion process for any given boundary.

In Section 2, we briefly review the method of images. We then establish the approximation methods for estimating the first hitting-time density or distribution of a Brownian motion process from any curved boundary by exploiting the use of images, which is referred to as the inverse method of images in Section 3. The inverse method of images produces an approximation to the boundary and the first hitting-time density of a Brownian motion process for this approximate boundary is to be found. Then the first hitting-time density for this approximate boundary is used as an approximation of the first hitting-time density for the boundary of interest. Therefore, the accuracy of this first hitting-time density approximation is very dependent on the accuracy of the approximate boundary. We shall discuss such dependence in Section 4. Numerical examples for both one-sided and two-sided boundary cases are given in Section 5.

2. The method of images

The method of images was first introduced by Daniels (1969) as a method of creating nonlinear boundaries with easily calculated first exit distribution for a Brownian motion process. It considers a variety of 'sources' distributed over the positive space axis at time zero according to a distribution F, and an extra source with unit mass at the origin. The sources are thought of as the starting positions of Brownian motion processes to which one attributes negative and positive weights distributed according to F and a single positive unit weight when starting at zero. The superposition of all these processes with positive and negative weights can be represented as some function of time t, $\psi(t)$, $t > 0$. Consider a Brownian

motion process starting at the origin, with absorption at the boundary. On the set $\{(x, t) : x \leqslant \psi(t), t > 0\}$, if ψ is continuous the method of images yields the distribution of that part of the Brownian motion which is not absorbed at the boundary. This can be described mathematically as follows.

Suppose that F is a σ-finite signed measure with

$$\int_0^\infty \phi(\sqrt{\varepsilon}\theta)|F(\mathrm{d}\theta)| < \infty, \qquad \forall \varepsilon > 0, \tag{1}$$

where ϕ is the density function of the standard normal distribution. Define the function

$$h(x, t) \equiv \frac{1}{\sqrt{t}}\phi\left(\frac{x}{\sqrt{t}}\right) - \frac{1}{a}\int_0^\infty \frac{1}{\sqrt{t}}\phi\left(\frac{x-\theta}{\sqrt{t}}\right)F(\mathrm{d}\theta), \tag{2}$$

for some real constant $a > 0$. Let

$$\psi(t) \equiv \inf\{x : h(x, t) < 0\}, \qquad t > 0. \tag{3}$$

Then h satisfies the *heat equation*

$$\frac{\partial h}{\partial t} = \frac{1}{2}\frac{\partial^2 h}{\partial x^2} \qquad \text{on } \mathbb{R} \times \mathbb{R}_+, \tag{4}$$

subject to boundary conditions (3) and

$$h(\cdot, 0) = \delta_0 \qquad \text{on } (-\infty, \psi(0+)], \tag{5}$$

where δ_0 is the Dirac measure at 0.

Let τ_ψ be the first exit time of W from ψ, so that

$$\tau_\psi \equiv \inf_{t>0}\{t : W_t \geqslant \psi(t)\}.$$

Since we have

$$W(t) > \psi(t) \Rightarrow h(W_t, t) \leqslant 0, \qquad t > 0,$$

and

$$h(W_t, t) < 0 \Rightarrow W_t \geqslant \psi(t), \qquad t > 0,$$

we obtain

$$\tau_\psi = \inf\{t > 0 : h(W_t, t) = 0\}.$$

We now present some results on the first hitting time. The following are taken from Lerche (1986, Chapter 1) and have been adapted to the notation used in this paper.

Theorem 2.1. *Suppose that W is a standard Brownian motion process, ψ is some boundary given by* (3)*, and τ is the first hitting time of W with respect to ψ such that*

$$\tau = \inf_{t>0}\{t : W_t \geqslant \psi(t)\}.$$

If ψ is continuous, then, on $C = \{(x, t) : x \leqslant \psi(t), t > 0\}$, the taboo density is given by

$$\frac{P(W(t) \in \mathrm{d}x,\ \tau > t)}{\mathrm{d}x} = h(x,\ t),$$

with

$$h(x,\ t) = \frac{1}{\sqrt{t}}\phi\left(\frac{x}{\sqrt{t}}\right) - \frac{1}{a}\int_0^\infty \frac{1}{\sqrt{t}}\phi\left(\frac{x-\theta}{\sqrt{t}}\right)F(\mathrm{d}\theta),$$

where ϕ and Φ are the density and distribution functions of a standard normal distribution respectively, and F is defined in (1).

Corollary 2.1. *The distribution and density of the time at which a Brownian motion W first exits the boundary ψ are, respectively,*

$$P(\tau \leqslant t) = 1 - \Phi\left(\frac{\psi(t)}{\sqrt{t}}\right) + \frac{1}{a}\int_0^\infty \Phi\left(\frac{\psi(t)-\theta}{\sqrt{t}}\right)F(\mathrm{d}\theta)$$

and

$$p(t) = \frac{\psi(t)}{2t^{3/2}}\phi\left(\frac{\psi(t)}{\sqrt{t}}\right) - \int_0^\infty \left(\frac{\psi(t)-\theta}{2t^{3/2}}\right)\phi\left(\frac{\psi(t)-\theta}{\sqrt{t}}\right)F(\mathrm{d}\theta).$$

3. Inverse method of images

The method of images constructs a boundary ψ from a given σ-finite measure F, and yields the corresponding boundary-crossing density or distribution. We now obtain a σ-finite measure F corresponding to $\tilde{\psi}$ which approximates a given boundary ψ, and from that obtain an approximation for the distribution of the first exit time of a Brownian motion process with respect to ψ.

3.1. Derivation of the method for one-sided boundaries

Our intention is to consider a class of boundaries obtained by applying the method of images to measures which can be written as sums of point masses. We estimate the distribution of images for a given curved boundary.

We have, from Section 2, the boundary condition

$$h(\psi(t),\ t) = 0, \qquad t > 0,$$

where, taking the normalizing constant $a = 1$,

$$h(x,\ t) = \frac{1}{\sqrt{t}}\phi\left(\frac{x}{\sqrt{t}}\right) - \int_0^\infty \frac{1}{\sqrt{t}}\phi\left(\frac{x-\theta}{\sqrt{t}}\right)F(\mathrm{d}\theta). \tag{6}$$

That is, for every value on the boundary $\psi(t)$, the measure $F(\mathrm{d}\theta)$ must satisfy

$$1 = \int_0^\infty F(\mathrm{d}\theta)\exp\left(\theta\frac{\psi(t)}{t} - \frac{\theta^2}{2t}\right), \qquad t > 0.$$

Furthermore, it can be shown (Lerche 1986) that if $\hat{\theta} = \inf\{y : F(0, y] > 0\} \geqslant 0$ then $\lim_{t\to 0}\psi(t) = \hat{\theta}/2$. This gives us $F(0, \theta] = 0$, for all $\theta < 2\lim_{t\to 0}\psi(t)$, so that it is sufficient to consider

$$1 = \int_{\hat{\theta}}^\infty F(\mathrm{d}\theta)\exp\left(\theta\frac{\psi(t)}{t} - \frac{\theta^2}{2t}\right), \qquad t > 0.$$

Now, suppose F is a collection of point masses, $\{F_r\delta_r\}_{1\leqslant r\leqslant N}$, where $N \in \mathbb{Z}^+$, and δ_r $(r = 1, \ldots, N)$ is the Dirac measure at point θ_r $(r = 1, \ldots, N)$. Then

$$1 = \int_0^\infty F_r\delta_r \exp\left(\theta\frac{\psi(t)}{t} - \frac{\theta^2}{2t}\right)\mathrm{d}t = \sum_{r=1}^N F_r \exp\left(\theta_r\frac{\psi(t)}{t} - \frac{\theta_r^2}{2t}\right), \qquad t > 0. \tag{7}$$

Now $\{F_r\}_{1\leqslant r\leqslant N}$ can be thought of as a collection of positive or negative point masses or weights which are attributed to Brownian motions with initial positions $\{\theta_r\}_{1\leqslant r\leqslant N}$ along the space axis. Equation (7) holds for all $t > 0$, and is true in particular for any collection of (positive) time points $0 < t_1 < t_2 < \ldots < t_s < \ldots < t_{2N}$. At these time points, we intend to ensure that ψ and the approximate boundary $\tilde{\psi}$ (corresponding to our approximate measure) are equal. This motivates the discretization of the above equation, which gives us a system of discretized equations for $\{\theta_r, F_r\}_{1\leqslant r\leqslant N}$ as follows:

$$1 = \sum_{r=1}^N F_r \exp\left(\theta_r\frac{\psi(t_s)}{t_s} - \frac{\theta_r^2}{2t_s}\right), \qquad s = 1, \ldots, 2N. \tag{8}$$

The inverse method of images proposed in (8) involves a system of *nonlinear* equations for $\{\theta_r, F_r\}_{1,\ldots,N}$. For certain boundaries, we may have some idea of the range of the θ_r (see Section 5.1.1), in which case we may preassign the values of the θ_r assuming $\theta_1 = \hat{\theta} = 2\lim_{t\to 0}\psi(t)$. The system of equations is then *linear* in the F_r. Only N equations are required to determine the F_r. In this case, an increase in the number of time points for interpolation may be required in order to preserve sufficient accuracy of the approximation, as there will be a loss of degrees of freedom in the fitting procedure due to the reduction of the number of parameters. However, the increase in the number of interpolation time points may cause the linear system for the F_r to become more singular.

3.2. Finding an approximate boundary

So $\{\theta_r, F_r\}_{1\leqslant r\leqslant N}$ can be considered as the distribution of the images along the (positive) space axis through the origin, with respect to which a solution $x = \tilde{\psi}(t)$ to $h(x, t) = 0$ is obtained using the method of images. Such a solution agrees with the boundary ψ at N time points $\{t_s\}_{1\leqslant s\leqslant N}$, and it may be considered an approximation to the true boundary ψ.

3.3. Estimating first hitting-time density and distribution

Applying the method of images, we obtain the exact first exit-time density and distribution corresponding to this approximate boundary $\tilde{\psi}$, as

$$\frac{\tilde{\psi}(t)}{2t^{3/2}}\phi\left(\frac{\tilde{\psi}(t)}{\sqrt{t}}\right) - \sum_{r=1}^{N} F_r\left(\frac{\tilde{\psi}(t)-\theta_r}{2t^{3/2}}\right)\phi\left(\frac{\tilde{\psi}(t)-\theta_r}{\sqrt{t}}\right), \qquad t>0, \tag{9}$$

and

$$1-\Phi\left(\frac{\tilde{\psi}(t)}{\sqrt{t}}\right) + \sum_{r=1}^{N} F_r\Phi\left(\frac{\tilde{\psi}(t)-\theta_r}{\sqrt{t}}\right), \qquad t>0, \tag{10}$$

respectively. Now if, for some T, $\sup_{0<t<T}|\tilde{\psi}(t)-\psi(t)|$ is sufficiently small, then we may approximate (9) and (10), for $0<t\leqslant T$, by

$$\frac{\psi(t)}{2t^{3/2}}\phi\left(\frac{\psi(t)}{\sqrt{t}}\right) - \sum_{r=1}^{N} F_r\left(\frac{\psi(t)-\theta_r}{2t^{3/2}}\right)\phi\left(\frac{\psi(t)-\theta_r}{\sqrt{t}}\right) \tag{11}$$

and

$$1-\Phi\left(\frac{\psi(t)}{\sqrt{t}}\right) + \sum_{r=1}^{N} F_r\Phi\left(\frac{\psi(t)-\theta_r}{\sqrt{t}}\right), \tag{12}$$

respectively, which will then be used as approximations of the first exit-time density and distribution for ψ. Thus the accuracy of the estimate of the first hitting-time density for ψ is strongly dependent on how close $\tilde{\psi}$ is to ψ. We shall discuss this in more detail in Section 4.

3.4. Connection with Daniels's refinements of tangent approximation

The method introduced in Section 2 is essentially an appropriate generalization of Daniels's (1996) refinements of the tangent approximation. Daniels used the method of images with two negative images at $2\alpha_1$, $2\alpha_2$, $(\alpha_1<\alpha_2)$, and with weights $F_r=\exp(-2\alpha_r\beta_r)$, $r=1, 2$, to obtain a curved boundary with an easily computable first exit-time distribution.

3.4.1. Daniels's first and second refinements

Daniels's first refinement (GTA1) suggests that the α_r and β_r are to be determined in such a way that the curved boundary so obtained interpolates the true boundary at the origin at zero degree, and at the first hitting time up to second-order derivatives of the boundary with respect to time. Let $\tilde{\xi}(u)=\psi/t$, with $u=1/t$; then the equations for the α_r and β_r are given by

$$\alpha_1 = \psi(0) = \tilde{\xi}_0',$$

$$\alpha_2 = \tilde{\xi}' - \frac{1}{2}\tilde{\xi}_0' + \left(\frac{1}{4}(\tilde{\xi}_0')^2 - \frac{1}{2}\frac{\tilde{\xi}''}{\tilde{\xi}' - \tilde{\xi}_0'}\right)^{1/2},$$

$$\beta_1 = \tilde{\xi} - \alpha_1 u - \frac{1}{2\alpha_1}\log\left(\frac{\alpha_2(\alpha_2 - \tilde{\xi}')}{(\alpha_2 - \alpha_1)(\alpha_1 + \alpha_2 - \tilde{\xi}')}\right),$$

$$\beta_2 = \tilde{\xi} - \alpha_2 u - \frac{1}{2\alpha_2}\log\left(\frac{\alpha_1(\tilde{\xi}' - \alpha_1)}{(\alpha_2 - \alpha_1)(\alpha_1 + \alpha_2 - \tilde{\xi}')}\right).$$

Daniels's second refinement (GTA2) suggests that the approximate boundary interpolates the true boundary up to the first derivative at both the origin and the first hitting time. The corresponding equations for the α_r and β_r are given by

$$\alpha_1 = \psi(0),$$

$$\beta_1 = \psi'(0),$$

$$\alpha_2(\tilde{\xi}' - \alpha_2) = \frac{\alpha_1(\alpha_1 - \tilde{\xi}')\exp(2\alpha_1(\tilde{\xi} - \alpha_1 u - \beta_1))}{1 - \exp(2\alpha_1(\tilde{\xi} - \alpha_1 u - \beta_1))},$$

$$\beta_2 = \tilde{\xi} - \alpha_2 u - \frac{1}{2\alpha_2}\log(1 - \exp(2\alpha_1(\tilde{\xi} - \alpha_1 u - \beta_1))).$$

3.4.2. Daniels's refinements for square root boundaries

There is evidence in the case of the square root boundary $l\sqrt{1+t}$, $l = 0.5, 1, 2$, that each of the refinements of the tangent approximation produces estimates of the first crossing-time density that are extremely close to the true density, and it appears to be more accurate than the estimate obtained from the tangent approximation (see Lo 1997, Appendix A). Furthermore, we observe that GTA2 tends to *over*estimate the true first hitting-time density, whereas GTA1 tends to *under*estimate the true first hitting-time density (see Lo 1997, Appendix A). This is due to the fact that the approximations to the square root boundaries via GTA1 and GTA2 *envelope* the exact boundary from below and above, respectively (see Roberts 1991, Theorem 2.8).

Thus an approximate boundary lying between the two boundaries corresponding to GTA1 and GTA2 can be associated with a more accurate estimation of the first hitting-time density in this case. One way to obtain such a boundary is to impose extra points of interpolation between the origin and the first hitting time. This can be achieved by the inverse method of images.

3.5. Approximation method for two-sided boundaries

The results on the method of images for one-sided boundaries from Section 2 can be extended to that for two-sided boundaries, $\psi = (\psi_+, \psi_-)$. When using the method of images for two-sided boundaries, instead of (2), we have the function

$$h(x, t) = \frac{1}{\sqrt{t}}\phi\left(\frac{x}{\sqrt{t}}\right) - \frac{1}{a}\int_{-\infty}^{\infty} \frac{1}{\sqrt{t}}\phi\left(\frac{x-\theta}{\sqrt{t}}\right) F(\mathrm{d}\theta), \tag{13}$$

where ϕ is the density function of standard normal distribution and F is a σ-finite signed measure having $\int_{-\infty}^{\infty} \phi(\sqrt{\varepsilon}\theta)|F(\mathrm{d}\theta)| < \infty$ for all $\varepsilon > 0$ and $F(\{0\}) = 0$. Expression (13) satisfies the heat equation (4) with boundary condition $h(\cdot, 0) = \delta_0$ on $(\psi_-(0+), \psi_+(0+))$, where

$$\psi_+(t) = \inf\{x > 0 : h(x, t) < 0, t > 0\}, \qquad \psi_-(t) = \sup\{x < 0 : h(x, t) < 0, t > 0\}.$$

An approximation for the first hitting-time density of a Brownian motion process for a two-sided boundary can be constructed using images similarly to that for a one-sided boundary. Here we have $h(\psi_+(t), t) = 0 = h(\psi_-(t), t)$, $t > 0$, where h is given by (13). Now, for any collection of time points $\{t_1 < t_2 < \ldots < t_N\}$, a system of discretized equations for F can be obtained similarly to (8) and is given by

$$1 = \sum_{r=1}^{2N} F_r \exp\left(\theta_r \frac{\psi_+(t_s)}{t_s} - \frac{\theta_r^2}{2t_s}\right), \qquad s = 1, \ldots, N;$$

$$1 = \sum_{r=1}^{2N} F_r \exp\left(\theta_r \frac{\psi_-(t_s)}{t_s} - \frac{\theta_r^2}{2t_s}\right), \qquad s = 1, \ldots, N.$$

With respect to the solution F_rs, we may construct a boundary $\tilde{\psi}_\pm = (\tilde{\psi}_+, \tilde{\psi}_-)$ using the method of images. These boundaries satisfy $\tilde{\psi}_+(t_s) = \psi_+(t_s)$ and $\tilde{\psi}_-(t_s) = \psi_-(t_s)$ for $1 \leqslant s \leqslant N$. Therefore, $\tilde{\psi}_\pm$ serves as an approximation to $\psi_\pm$, and the associated first hitting-time density or distribution can be used as an estimate of that for $\psi_\pm$.

3.6. Inverse method of images in practice

The approximation method which we described earlier in this section is simple yet extremely accurate and useful for general boundary-crossing problems of a Brownian motion process. However, for some boundaries which change more rapidly within the time interval of interest, the estimation may be sensitive to the locations for the images to be added and to the interpolation time points in the inversion procedure. In this case, we may consider adding a linear term to the boundary and work with the boundary $\psi(t) + \nu t$, $t > 0$ ($\nu \in \mathbb{R}$), instead. For a given boundary, we can use this method to make the new boundary more linear in the time interval of interest, and hence the system (8) becomes less sensitive to the interpolation time points.

Now the first crossing-time problem of a standard Brownian motion process W with respect to the boundary $\psi(t),\ t > 0$, can be considered as the problem of a Brownian motion process with drift ν, W^{ν}, with respect to the boundary $\psi(t) + \nu t,\ t > 0$. We may obtain an estimate of the first hitting-time density or distribution of W with respect to $\psi(t) + \nu t,\ t > 0$, using the inverse method of images, then make use of the Cameron–Martin–Girsanov formula to obtain the corresponding estimation for the problem of W^{ν} with respect to $\psi(t) + \nu t,\ t > 0$. The transformed boundary may be considered when the estimation is sensitive to the locations for the images to be added and to the interpolation time points in the inversion procedure.

4. Error analysis

In this section, we examine the accuracy of the estimates of the first hitting-time density or distribution which are produced by the inverse method of images. The approach produces an approximation $\tilde{\psi}$ for ψ, and the first hitting-time density of a Brownian motion for this approximate boundary is to be found. The first hitting-time density associated with $\tilde{\psi}$ is used as an approximation of that associated with ψ. The accuracy of this first hitting-time density approximation depends, therefore, very much on how close $\tilde{\psi}$ is to ψ. We write $\tilde{\psi}(s) = \psi(s) + \varepsilon(s),\ s > 0$.

Theorem 4.1. *Suppose that ψ is a one-sided boundary, $\tilde{\psi}$ is an approximation to ψ and $\bar{\varepsilon}_t = \sup_{0<s<t} |\tilde{\psi}(s) - \psi(s)|$. Let $k_t = \sup_{0<s<t} \mathrm{d}\psi(s)/\mathrm{d}s$, $\psi_1(s) = \psi(s) - \bar{\varepsilon}_t,\ 0 < s < t$, and p_{ψ} be the first hitting-time density of a standard Brownian motion process with respect to ψ. Then the following three statements hold:*

(*i*)
$$|P(\tau_{\psi} < t) - P(\tau_{\tilde{\psi}} < t)| \to 0 \qquad \text{as } \bar{\varepsilon}_t \downarrow\downarrow 0,$$
where $\tau_{\psi} = \inf\{s > 0,\ W(s) \geqslant \psi(s)\}$ and W is a standard Brownian motion process.

(*ii*) *Furthermore, for any $t > 0$,*
$$\limsup_{\bar{\varepsilon}_t \downarrow\downarrow 0} \left| \frac{P(\tau_{\psi} < t) - P(\tau_{\tilde{\psi}} < t)}{\bar{\varepsilon}_t} \right| \leqslant M,$$
where
$$M = 4\left| \int_0^t p_{\psi_1}(s) \left[\frac{\phi(k_t\sqrt{t-s})}{\sqrt{t-s}} + k_t \Phi(k_t\sqrt{t-s}) \right] \mathrm{d}s \right|.$$

(*iii*) *For any $t > 0$, if $p_{\psi_1}(s)$ is uniformly bounded on $(t - \gamma_t, t]$ for some $0 < \gamma_t < t$, then*
$$|P(\tau_{\psi} < t) - P(\tau_{\tilde{\psi}} < t)| \leqslant K\bar{\varepsilon}_t,$$

where

$$K = \begin{cases} 4\left(|k_t| + \dfrac{p^*}{|k_t|} + \displaystyle\int_0^t p_{\psi_1}(s)\phi\left(\frac{k_t}{2}\sqrt{t-s}\right) \Big/ (\sqrt{t-s})\mathrm{d}s \right) & \text{if } |k_t| > 0, \\ 4\left(p^{**} + \displaystyle\int_0^t p_{\psi_1}(s)\phi\left(\frac{1}{2}\sqrt{t-s}\right) \Big/ (\sqrt{t-s})\mathrm{d}s \right) & \text{if } k_t = 0, \end{cases}$$

in which $p^* = \sup_{s\in[t-4\bar{\varepsilon}_t/|k_t|,t]} p\psi_1(s)$ *with* $\bar{\varepsilon}_t < |k_t|\gamma_t/4$, *and* $p^{**} = \sup_{s\in[t-4\bar{\varepsilon}_t,t]} p_{\psi_1}(s)$ *with* $\bar{\varepsilon}_t < \gamma_t/4$.

Proof. (i) Define

$$\psi_2(s) = \psi(s) + \bar{\varepsilon}_t, \qquad 0 < s < t,$$

and

$$l_t(u) = \psi(s) + \bar{\varepsilon}_t + k_t(u-s), \qquad 0 < s \leqslant u < t.$$

We therefore have

$$\psi_1(s) \leqslant \tilde{\psi}(s) \leqslant \psi_2(s), \qquad 0 < s < t,$$

and

$$\psi_1(s) \leqslant \psi(s) \leqslant \psi_2(s), \qquad 0 < s < t.$$

Now

$$\begin{aligned} & P(\tau_{\psi_1} < t) - P(\tau_{\psi_2} < t) \\ &= \int_0^t p_{\psi_1}(s)(1 - P(s < \tau_{\psi_2} < t | W_s = \psi_1(s), \tau_{\psi_2} > s))\mathrm{d}s \\ &\leqslant \int_0^t p_{\psi_1}(s)(1 - P(s < \tau_{1_t} < t | W_s = \psi_1(s), \tau_{\psi_2} > s))\mathrm{d}s \\ &= \int_0^t p_{\psi_1}(s)\left\{ \Phi\left(\frac{2\bar{\varepsilon}_t + k_t(t-s)}{\sqrt{t-s}}\right) - \mathrm{e}^{-4\bar{\varepsilon}_t k_t}\Phi\left(\frac{k_t(t-s) - 2\bar{\varepsilon}_t}{\sqrt{t-s}}\right)\right\}\mathrm{d}s \\ &\xrightarrow{\bar{\varepsilon}_t \downarrow\downarrow 0} 0. \end{aligned} \tag{15}$$

(ii) Furthermore, by letting

$$I(\bar{\varepsilon}_t) = \int_0^t p_{\psi_1}(s)\left\{ \Phi\left(\frac{2\bar{\varepsilon}_t + k_t(t-s)}{\sqrt{t-s}}\right) - \mathrm{e}^{-4\bar{\varepsilon}_t k_t}\Phi\left(\frac{k_t(t-s) - 2\bar{\varepsilon}_t}{\sqrt{t-s}}\right)\right\}\mathrm{d}s,$$

we take

$$M = \left| \frac{\mathrm{d}I}{\mathrm{d}\bar{\varepsilon}_t}\Big|_{\bar{\varepsilon}_t \downarrow 0} \right| = 4\left| \int_0^t p_{\psi_1}(s)\left[\frac{\phi(k_t\sqrt{t-s})}{\sqrt{t-s}} + k_t\Phi(k_t\sqrt{t-s})\right]\mathrm{d}s \right|.$$

(iii) Let $I(\bar{\varepsilon}_t) = I_1(\bar{\varepsilon}_t) + I_2(\bar{\varepsilon}_t)$, with

$$I_1(\bar{\varepsilon}_t) = \int_0^t p_{\psi_1}(s)\left\{\Phi\left(\frac{2\bar{\varepsilon}_t + k_t(t-s)}{\sqrt{t-s}}\right) - \Phi\left(\frac{k_t(t-s) - 2\bar{\varepsilon}_t}{\sqrt{t-s}}\right)\right\}\mathrm{d}s$$

and

$$I_2(\bar{\varepsilon}_t) = \int_0^t p_{\psi_1}(s)(1 - \mathrm{e}^{-4\bar{\varepsilon}_t k_t})\Phi\left(\frac{k_t(t-s) - 2\bar{\varepsilon}_t}{\sqrt{t-s}}\right)\mathrm{d}s.$$

We have $I_2(\bar{\varepsilon}_t) \leqslant 4\bar{\varepsilon}_t|k_t|$ since $1 - \mathrm{e}^{-4\bar{\varepsilon}_t k_t} \leqslant 4\bar{\varepsilon}_t|k_t|$. Now consider I_1 for $|k_t| > 0$. Let $u = k_t\sqrt{t-s}$ and split the integral into two parts as

$$I_1(\bar{\varepsilon}_t) = \int_0^{2\sqrt{\bar{\varepsilon}_t|k_t|}} + \int_{2\sqrt{\bar{\varepsilon}_t|k_t|}}^{|k_t|t^{1/2}} \frac{2u}{k_t^2} p_{\psi_1}\left(t - \frac{u^2}{k_t^2}\right)\left\{\Phi\left(u + \frac{2\bar{\varepsilon}_t k_t}{u}\right) - \Phi\left(u - \frac{2\bar{\varepsilon}_t k_t}{u}\right)\right\}\mathrm{d}u$$

$$= I_1^{(1)}(\bar{\varepsilon}_t) + I_1^{(2)}(\bar{\varepsilon}_t),$$

say. We also have

$$I_1^{(1)}(\bar{\varepsilon}_t) \leqslant \frac{2p^*}{k_t^2}\int_0^{2\sqrt{\bar{\varepsilon}_t|k_t|}} u\,\mathrm{d}u = \frac{4\bar{\varepsilon}_t p^*}{|k_t|}$$

and

$$I_1^{(2)}(\bar{\varepsilon}_t) \leqslant \frac{8\bar{\varepsilon}_t}{|k_t|}\int_0^{k_t t^{1/2}} \frac{1}{\sqrt{2\pi}}\,\mathrm{e}^{-u^2/8} p_{\psi_1}\left(t - \frac{u^2}{k_t^2}\right)\mathrm{d}u$$

since $\Phi(u + (2\bar{\varepsilon}_t k_t)/u) - \Phi(u - (2\bar{\varepsilon}_t k_t)/u) \leqslant (4\bar{\varepsilon}_t k_t)/(u\sqrt{2\pi})\mathrm{e}^{-u^2/8}$ for $u \geqslant 2\sqrt{\bar{\varepsilon}_t|k_t|}$. Therefore,

$$I(\bar{\varepsilon}_t) \leqslant 4\left(|k_t| + \frac{p^*}{|k_t|} + \int_0^t p_{\psi_1}(s)\frac{\phi([k_t/2]\sqrt{t-s})}{\sqrt{t-s}}\,\mathrm{d}s\right)\bar{\varepsilon}_t.$$

Similarly, for $k_t = 0$, we have, by letting $u = \sqrt{t-s}$,

$$I(\bar{\varepsilon}_t) = \left(\int_0^{2\sqrt{\bar{\varepsilon}_t}} + \int_{2\sqrt{\bar{\varepsilon}_t}}^{t^{1/2}}\right) 2up_{\psi_1}(t-u^2))\left\{\Phi\left(\frac{2\bar{\varepsilon}_t}{u}\right) - \Phi\left(-\frac{2\bar{\varepsilon}_t}{u}\right)\right\}$$

$$\leqslant 4\left(p^{**} + \int_0^t p_{\psi_1}(s)\frac{\phi(\frac{1}{2}\sqrt{t-s})}{\sqrt{t-s}}\mathrm{d}s\right)\bar{\varepsilon}_t.$$

□

This result readily extends to two-sided boundaries as follows.

Corollary 4.1. *Suppose that* $\psi_\pm = (\psi_+, \psi_-)$ *is a two-sided boundary with* $\psi_-(0) <$

$0 < \psi_+(0)$ and $\psi_-(s) < \psi_+(s)$, $0 < s < T$, that $\tilde{\psi}_\pm = (\tilde{\psi}_+, \tilde{\psi}_-)$ is an approximation of $\psi_\pm$, and that

$$\bar{\varepsilon}_t^+ = \sup_{0<s<t} |\tilde{\psi}_+(s) - \psi_+(s)|,$$

$$\bar{\varepsilon}_t^- = \sup_{0<s<t} |\tilde{\psi}_-(s) - \psi_-(s)|$$

with $\bar{\varepsilon}_t = \bar{\varepsilon}_t^+ \vee \bar{\varepsilon}_t^-$. Let $k_t^+ = \sup_{0<s<t} \mathrm{d}\psi_+(s)/\mathrm{d}s$, $k_t^- = \inf_{0<s<t} \mathrm{d}\psi_-(s)/\mathrm{d}s$, $\psi_\pm^{(1)} = (\psi_+^{(1)}, \psi_-^{(1)})$ with $\psi_+^{(1)}(s) = \psi_+(s) - \bar{\varepsilon}_t$ $(0 < s < t)$, $\psi_-^{(1)}(s) = \psi_-(s) + \bar{\varepsilon}_t$ $(0 < s < t)$, and p_ψ be the first hitting-time density of a standard Brownian motion process with respect to ψ. Then the following statements hold:

(*i*)

$$|P(\tau_{\psi_\pm} < t) - P(\tau_{\tilde{\psi}_\pm} < t)| \to 0 \qquad \text{as } \bar{\varepsilon}_t \downarrow\downarrow 0,$$

where

$$\tau_{\psi_\pm} = \inf\{s > 0,\ W(s) \geqslant \psi_+(s) \text{ or } W(s) \leqslant \psi_-(s)\}$$

and W is a standard Brownian motion process.

(*ii*) *Furthermore, for any $t > 0$,*

$$\limsup_{\bar{\varepsilon}_t \downarrow\downarrow 0} \left| \frac{P(\tau_{\psi_\pm} < t) - P(\tau_{\tilde{\psi}_\pm} < t)}{\bar{\varepsilon}_t} \right| \leqslant M',$$

where

$$M' = 4\left\{ \left| \int_0^t p_{\psi_+^{(1)}}(s) \left[\frac{\phi(k_t^+\sqrt{t-s})}{\sqrt{t-s}} + k_t^+ \Phi(k_t^+\sqrt{t-s}) \right] \mathrm{d}s \right| \right.$$

$$\left. + \left| \int_0^t p_{\psi_-^{(1)}}(s) \left[\frac{\phi(-k_t^-\sqrt{t-s})}{\sqrt{t-s}} - k_t^- \Phi(-k_t^-\sqrt{t-s}) \right] \mathrm{d}s \right| \right\}.$$

(*iii*) *For any $t > 0$, if $p_{\psi_\pm^{(1)}}(s)$ is uniformly bounded on $(t - \gamma_t, t]$ for some $0 < \gamma_t < t$, then*

$$|P(\tau_{\psi_\pm} < t) - P(\tau_{\tilde{\psi}_\pm} < t)| = (K'_+ + K'_-)\bar{\varepsilon}_t,$$

where

$$K'_\pm = \begin{cases} 4\left(|k_t^\pm| + \dfrac{p_\pm^*}{|k_t^\pm|} + \displaystyle\int_0^t p_{\psi_\pm^{(1)}}(s)\phi\left(\frac{\pm k_t^\pm}{2}\sqrt{t-s}\right) \Big/ (\sqrt{t-s})\mathrm{d}s \right) & \text{if } |k_t^\pm| > 0, \\ 4\left(p_\pm^{**} + \displaystyle\int_0^t p_{\psi_\pm^{(1)}}(s)\phi\left(\tfrac{1}{2}\sqrt{t-s}\right)/(\sqrt{t-s})\mathrm{d}s \right) & \text{if } k_t^\pm = 0, \end{cases}$$

in which $p_\pm^* = \sup_{s\in[t-4\bar{\varepsilon}_t/|k_t^\pm|,t]} p_{\psi_\pm^{(1)}}(s)$ with $\bar{\varepsilon}_t < |k_t^\pm|\gamma_t/4$, and $p_\pm^{**} = \sup_{s\in[t-4\bar{\varepsilon}_t,t]} p_{\psi_\pm^{(1)}}(s)$ with $\bar{\varepsilon}_t < \gamma_t/4$.

Proof. The proof is similar to that of Theorem 4.1. We define $\psi_{\pm}^{(2)} = (\psi_{+}^{(2)}, \psi_{-}^{(2)})$, with

$$\psi_{+}^{(2)}(s) = \psi_{+}(s) + \bar{\varepsilon}_t, \qquad 0 < s < t,$$

$$\psi_{-}^{(2)}(s) = \psi_{-}(s) - \bar{\varepsilon}_t, \qquad 0 < s < t,$$

and

$$l_t(u)^{+} = \psi_{+}^{(2)}(s) + k_t^{+}(u-s) = \psi_{+}(s) + \bar{\varepsilon}_t + k_t^{+}(u-s), \qquad 0 < s \leqslant u < t,$$

$$l_t(u)^{-} = \psi_{-}^{(2)}(s) + k_t^{-}(u-s) = \psi_{-}(s) - \bar{\varepsilon}_t + k_t^{-}(u-s), \qquad 0 < s \leqslant u < t.$$

We have

$$P(\tau_{\psi_{\pm}^{(1)}} < t) - P(\tau_{\psi_{\pm}^{(2)}} < t) = \left[P(\tau_{\psi_{+}^{(1)}} < t) + P(\tau_{\psi_{-}^{(1)}} < t) - P(\tau_{\psi_{+}^{(1)}} < t,\, \tau_{\psi_{-}^{(1)}} < t)\right]$$
$$- \left[P(\tau_{\psi_{+}^{(2)}} < t) + P(\tau_{\psi_{-}^{(2)}} < t) - P(\tau_{\psi_{+}^{(2)}} < t,\, \tau_{\psi_{-}^{(2)}} < t)\right].$$

Now

$$\{\tau_{\psi_{+}^{(2)}} < t,\, \tau_{\psi_{-}^{(2)}} < t\} \subset \{\tau_{\psi_{+}^{(1)}} < t,\, \tau_{\psi_{-}^{(1)}} < t\}$$

and so

$$P(\tau_{\psi_{+}^{(2)}} < t,\, \tau_{\psi_{-}^{(2)}} < t) \leqslant P(\tau_{\psi_{+}^{(1)}} < t,\, \tau_{\psi_{-}^{(1)}} < t).$$

It follow that

$$P(\tau_{\psi_{\pm}^{(1)}} < t) - P(\tau_{\psi_{\pm}^{(2)}} < t) \leqslant [P(\tau_{\psi_{+}^{(1)}} < t) + P(\tau_{\psi_{-}^{(1)}} < t)] - [P(\tau_{\psi_{+}^{(2)}} < t) + P(\tau_{\psi_{-}^{(2)}} < t)],$$

and

$$|P(\tau_{\psi_{\pm}^{(1)}} < t) - P(\tau_{\psi_{\pm}^{(2)}} < t)| \leqslant |P(\tau_{\psi_{+}^{(1)}} < t) - P(\tau_{\psi_{+}^{(2)}} < t)| + |P(\tau_{\psi_{-}^{(1)}} < t) - P(\tau_{\psi_{-}^{(2)}} < t)|.$$

The proof now follows from the results in Theorem 4.1. □

5. Numerical examples

5.1. Boundary crossing problems with one-sided boundaries

We apply the inverse method of images or delayed images to the square root boundary $l\sqrt{1+t}$ ($l \in \mathbb{R}_+$; $t > 0$) and the parabolic boundary $b + at - ct^2$ ($b, c, a \in \mathbb{R}$; $t > 0$). The resulting first hitting-time density approximations will be compared to the true density for the corresponding boundary.

Keilson and Ross (1975) tabulated the probability for a standard Ornstein–Uhlenbeck process to cross a horizontal boundary of height l before time s. From these times, setting $t = \frac{1}{2}\log(1+s)$ gives the probability of Brownian motion crossing the square root boundary $l\sqrt{1+s}$, $s > 0$, before time t. As suggested by Daniels (1996), numerical differentiation

then produces the first hitting-time density. (The table produced by Keilson and Ross is accurate to four decimal places only, which leads to inaccuracies after interpolation and differentiation.) For parabolic boundary problems with $c > 0$, we have compared our approximations to the exact solutions produced by Dhlakama (1994) who expressed the density of a Brownian motion process first hitting the parabolic boundary $b + at - ct^2$ (b, $c > 0$, $a \in \mathbb{R}$; $t > 0$) in terms of Airy functions.

In some cases, we may use the L^1 quantity

$$D_t = \int_0^t |\tilde{p}(s) - p(s)| \mathrm{d}s, \tag{14}$$

where $p(s)$, $0 < s \leqslant t$, is the true first hitting-time density at s and $\tilde{p}(s)$ is an estimate of $p(s)$, $0 < s \leqslant t$, to measure the discrepancy between the approximate density and the true density.

5.1.1. Square-root boundary

For the square-root boundary $l\sqrt{1+t}$ ($l = 0.5, 1, 2$), we apply the inverse method of images with some preassigned values of θ_r to obtain estimates of F_r. Then an estimate of the first hitting-time density or distribution can be obtained from the estimated values of F_r using the method of images.

Choice of interpolation methods and thetas. The number of time points at which the approximate boundary interpolates the true boundary is equal to the number of θ_r introduced. Furthermore, the interpolation time points $\{t_r\}_{1,\ldots,N}$ ($0 = t_1 < t_2 < \ldots < t_N = t$, $t > 0$) are to be taken as equally spaced in the time interval $(0, t]$ for each boundary-crossing problem.

The values of α from GTA1 and GTA2 (Section 3.4.1) provide us with some idea of the θs in the inversion procedure of the method of images. Let $\alpha_r^{(j)}$, $r = 1, 2$, denote the values of α obtained under GTAj, $j = 1, 2$. In the case of square root boundaries, GTA1 produces an approximate boundary which bounds the true boundary from below prior to the first exit time, whereas with GTA2 the corresponding approximate boundary bounds the true boundary from above prior to the first exit time. We therefore expect that the values of α associated with the true boundary lie between those from GTA1 and GTA2. With this in mind, when using the inverse method of images in the approximation of the first hitting-time density for the square root boundary in the time interval $(0, t]$, we let the values of $\{\theta_r\}_{1,\ldots,N}$ be $\{2\alpha_1, 2\overline{\alpha}_2(t_r), r = 2, \ldots, N\}$, where $\overline{\alpha}_2$ is the average of the values of $\alpha_2^{(j)}$, $j = 1, 2$.

In this example, we consider the first hitting-time density approximation in the time interval $(0, 2.4]$ for $0.5\sqrt{1+t}$, $t > 0$, and that in $(0, 6]$ for $\sqrt{1+t}$, $t > 0$, using five interpolation points in the corresponding time interval of interest (see Table 1). In the case $2\sqrt{1+t}$, $t > 0$, we use six interpolation points for approximation in the time interval $(0, 10]$ (see Table 1). Indeed, for each of these boundaries, three-point interpolations produce a fairly good approximation to the corresponding boundary, and hence a reasonably accurate approximation for the corresponding first hitting-time density. Accuracy of the approximations is improved when five or six interpolation points are used instead.

Table 1. Interpolations, θs and Fs used in the inverse method of images for square root and parabolic boundaries

ψ	Interpolation points θs		Fs
$0.5\sqrt{1+t}$, $t>0$	0.01, 0.61, 1.21, 1.80, 2.40	1.00, 1.81, 2.20, 2.48, 2.71	0.78, 0.07, 0.090, −0.34, 0.28
$\sqrt{1+t}$, $t>0$	0.01, 1.51, 3.01, 4.50, 6.00	2.00, 3.14, 3.78, 4.30, 4.74	0.37, 0.20, 0.16, −0.64, 0.53
$2\sqrt{1+t}$, $t>0$	0.01, 2.01, 4.01, 6.00, 8.00, 10.00	4.00, 5.25, 6.26, 7.14, 7.92, 8.64	0.02, 0.15, −0.42, 0.91, −0.95, 0.44
$0.5-0.5t^2$, $t>0$	0.01, 0.41, 0.81, 1.20, 1.60, 2.00	1.00, 1.83, 2.62, 3.62, 4.86, 6.40	1.01, 1.77, −3.03, 1.12×10^2, -9.61×10^2, 1.01×10^6
$0.5+8t+0.5t^2$, $t>0$	0.005, 0.30, 0.60, 0.90, 1.20, 1.50	1.00, 1.50, 1.66, 1.62, 1.44, 1.14	0.00033, 0.0036, 0.00073, −0.0015, −0.0033, 0.00099

Increasing the number of interpolation points would produce a more accurate approximate boundary for the corresponding problem; however, this may cause the system (8) to become almost singular when more than about seven interpolation points are introduced.

Refining the time interval for estimations. One way to improve the approximation of the first hitting-time density or distribution in $(0, t]$ is to refine the time interval over which the estimation takes place, say, $0 = t_{N_1} < t_{N_2} < \ldots < t_{N_n} = t$. That is, for each time interval $(0, t_{N_i}]$, $2 \leqslant i \leqslant n$, we have an approximate boundary $\tilde{\psi}_{t_{N_i}}$ constructed by the inverse method of images. Each approximate boundary $\tilde{\psi}_{t_{N_i}}$, $2 \leqslant i \leqslant n$, agrees with ψ, say, at N points in the time interval $(0, t_{N_i}]$. Generally the $\tilde{\psi}_{t_{N_i}}$ approximate ψ more accurately than the $\tilde{\psi}_{t_{N_j}}$ in the time interval $(0, t_{N_i}]$ for $2 \leqslant i < j \leqslant n$, in which case we approximate the first hitting-time density for ψ in $(0, t_{N_i}]$ by that corresponding to $\tilde{\psi}_{t_{N_i}}$.

Let $\tilde{p}(\cdot|t_{N_i})$, $2 \leqslant i \leqslant n$, denote the density of a Brownian motion process which first exits the approximate boundary $\tilde{\psi}_{t_{N_i}}$ in the time interval $(0, t_{N_i})$. Then the first hitting-time density can be used as an approximation of that corresponding to ψ in the time interval $(0, t_N i)$. Therefore an approximation of the first hitting-time density for a Brownian motion process with respect to ψ at $s \in (0, t]$ is given by

$$\tilde{p}(s) = \sum_{i=2}^{n} \tilde{p}(s|t_{N_i}) I(s \in (t_{N_{i-1}}, t_{N_i}]), \qquad 0 < s \leqslant t,$$

where $I(s \in (t_{N_{i-1}}, t_{N_i}])$ is an indicator function taking the value 1 if $s \in (t_{N_{i-1}}, t_{N_i}]$, and 0 otherwise. The corresponding approximation, $\tilde{P}$, for the first hitting-time distribution is given by

$$\tilde{P}(s) = \sum_{i=2}^{n} \tilde{P}(s|t_{N_i}) I(s \in (t_{N_{i-1}}, t_{N_i}]), \qquad 0 < s \leqslant t,$$

where $\tilde{P}(\cdot|t_{N_i})$, $2 \leqslant i \leqslant n$, is the first hitting distribution of a Brownian motion process to the

approximate boundary $\tilde{\psi}_{t_{N_i}}$ in the time interval $(0, t_{N_i})$. We note that there could be jumps in $\tilde{p}(s)$ $(0 < s \leqslant t)$ at the t_{N_i}.

Approximation results. The first hitting-time density estimation using the inverse method of images is extremely good for boundaries $l\sqrt{1+t}$, $l = 0.5, 1, 2$ (see Table 1 for the corresponding θ_r and F_r). The density estimates are virtually indistinguishable from the true densities for each of these cases. This is due to the accuracy of the corresponding boundary as an approximation to the true boundary. Figures 1–3 show the first hitting-time density

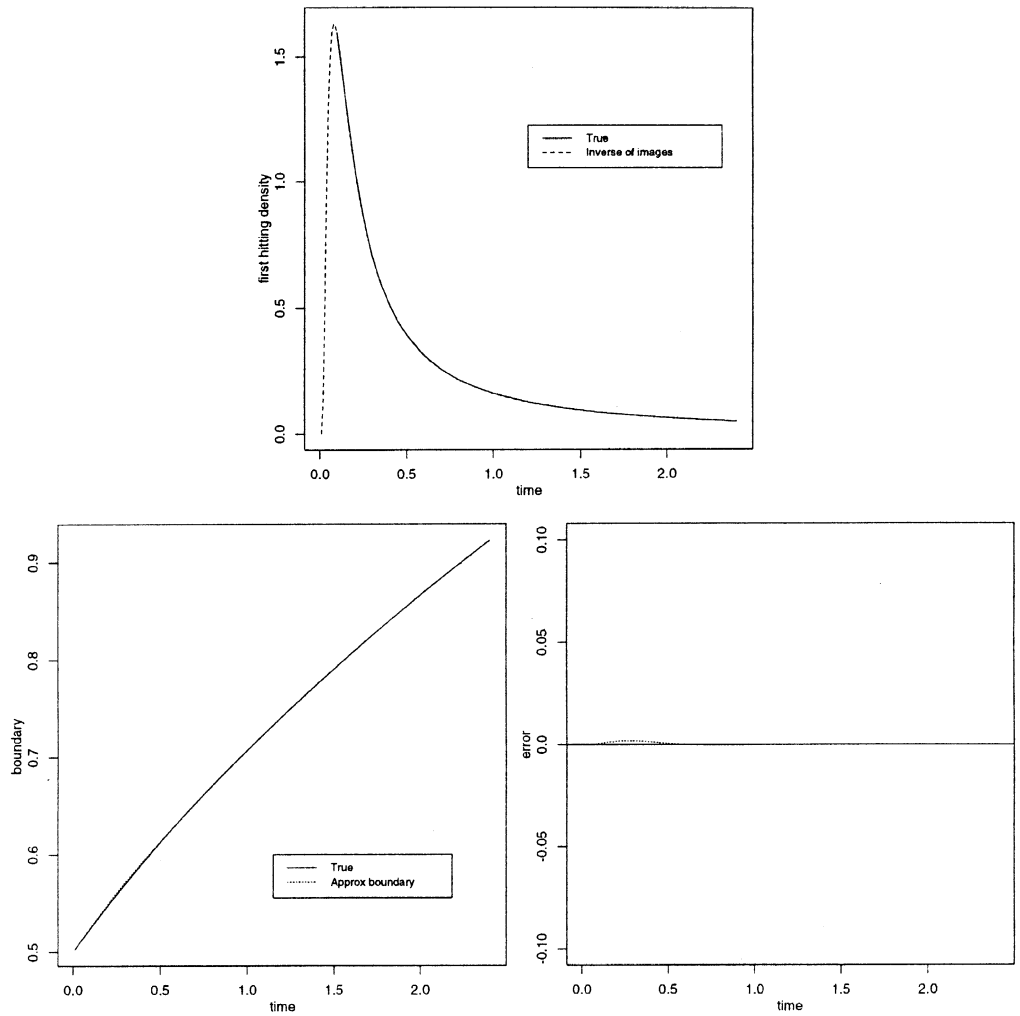

Figure 1. First hitting-time density approximation for $0.5\sqrt{1+t}$ (top) by the inverse method of images. Approximate boundary (bottom left) and deviance of the approximate boundary from the true boundary (bottom right).

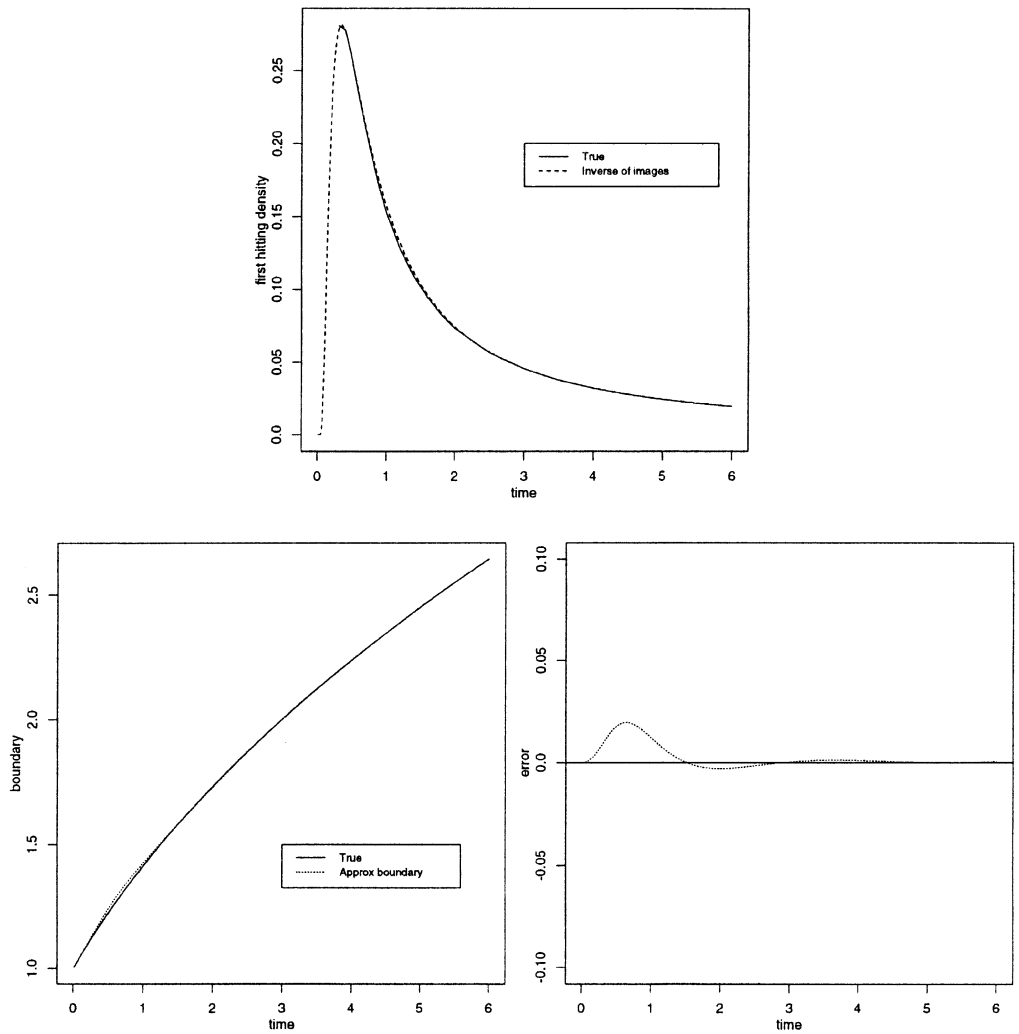

Figure 2. First hitting-time density approximation for $\sqrt{1+t}$ (top) by the inverse method of images. Approximate boundary (bottom left) and deviance of the approximate boundary from the true boundary (bottom right).

approximations for the square root boundaries under consideration (top) and the corresponding approximate boundaries and the deviance of these approximate boundaries from the corresponding true boundaries (bottom). For the boundary $2\sqrt{1+t}$, $t > 0$, the inverse method of images gives $M = 0.3898$ and $\overline{\epsilon}_{10} = 0.054\,28$ (see Lemma 4.1 for the definition of M and $\overline{\epsilon}$), and hence the absolute error of the first hitting distribution approximation in

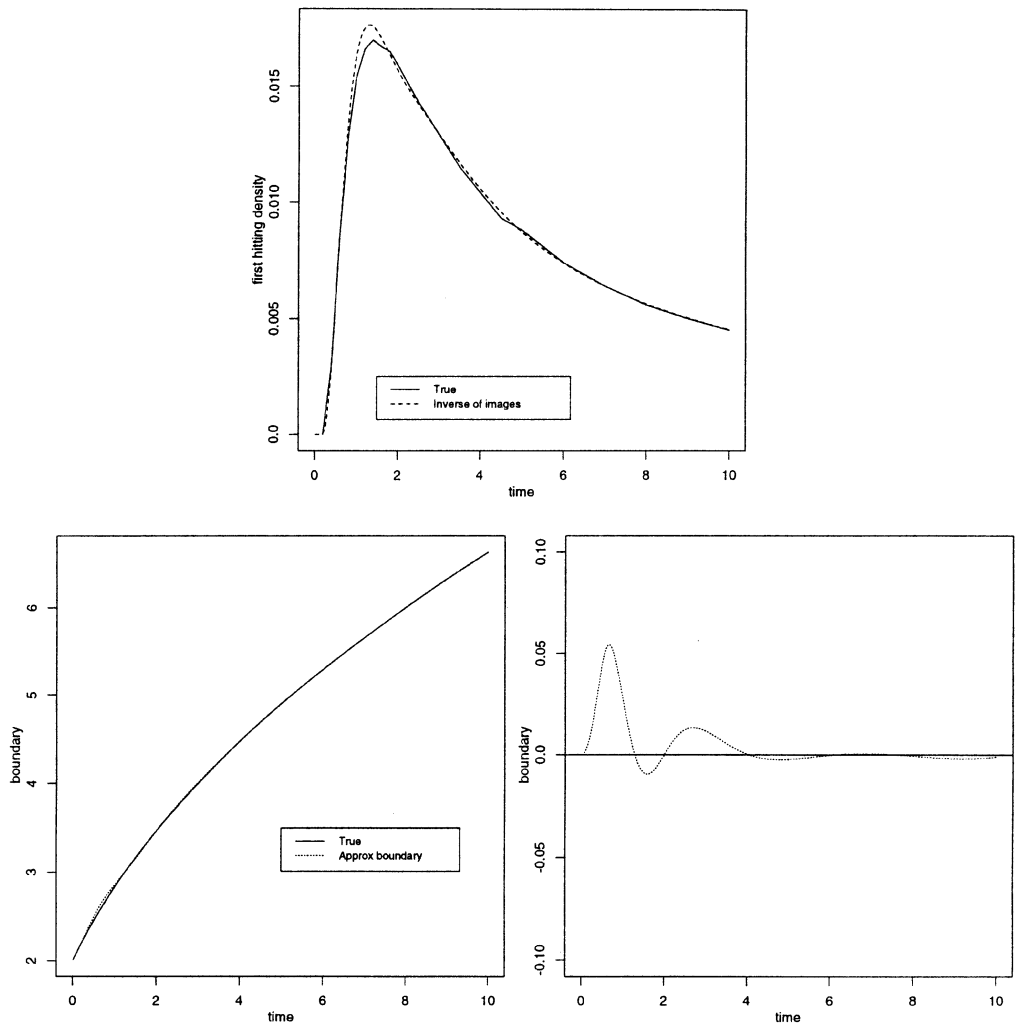

Figure 3. First hitting-time density approximation for $2\sqrt{1+t}$ (top) by the inverse method of images. Approximate boundary (bottom left) and deviance of the approximate boundary from the true boundary (bottom right).

the time interval $(0, 10]$ is less than $0.021\,16$, that is, $\sup_{0<t\leqslant 10}|P(\tau_\psi < t) - P(\tau_{\tilde{\psi}} < t)| \leqslant 0.021\,16$.

Comparing with Daniels's refinements for the boundary $2\sqrt{1+t}$, $t > 0$ – see Figure 3 and Lo's (1997) Figure A.3 – the inverse method of images produces a more accurate density approximation in the time interval (0, 10], except in the interval (1, 2). However, we

can improve the accuracy of the first hitting-time density approximations by refining the time interval over which the estimation takes place (see Table 2). In the case $\psi(t) = 2\sqrt{1+t},\ t > 0$, where the first hitting-time density approximation in the time interval (0, 10] is considered, we have refined time intervals of (0, 3], (0, 5] and (0, 10]. Five interpolation points are used for each of the refined time intervals. The first hitting-time density approximation so obtained is extremely accurate, which can be seen from Figure 4 (top). This is explained by the improved accuracy of the corresponding approximate boundary (see Figure 4 (bottom)).

We may also compare Figure 3 with Figure 4 to see the improvement of the approximate boundary and that of the associated first hitting-time density approximation by refining the time interval. Indeed, the approximation with refined time intervals has $D_{10} \approx 0.000\,699\,4$ (see (14) for the definition of D_t) which is smaller than 0.001 291, the value corresponding to the approximation without refined intervals. That is, the first hitting-time density approximation with refined time intervals has less discrepancy from the true density in this example. Furthermore, with refined time intervals, we have $\sup_{0<t\leqslant 10} |P(\tau_\psi < t) - P(\tau_{\tilde{\psi}} < t)| \leqslant 0.005\,19$, which is smaller than it would be without refined time intervals.

5.1.2. Parabolic boundary

We now consider the first hitting-time density approximation for the parabolic boundary $\psi(t) = b - ct^2,\ t > 0$, using the inverse method of images. Since the first crossing-time distribution or density of a standard Brownian motion process with respect to any boundary of the form $\psi(t) = b + at - ct^2,\ t > 0$, is equal to the first crossing-time distribution or density of a Brownian motion process with drift $-a$ with respect to the boundary $b - ct^2$ $(t > 0)$, we can apply the Cameron–Martin–Girsanov formula to give

$$p_{-a}(t) = \exp(-a\psi(t) - \tfrac{1}{2}a^2 t)p_0(t),$$

where p_{-a} and p_0 are the first boundary-crossing densities of Brownian motion with drift $-a$ and without drift respectively, to obtain the first hitting-time density approximation for the boundary $b + at - ct^2$ $(t > 0)$ from that for the boundary $b - ct^2$ $(t > 0)$ or vice versa.

Table 2. Interpolations, θs and Fs used in the inverse method of images with refined time intervals for $2\sqrt{1+t}$

Time range	Interpolation points	θs	Fs
(0.0, 3.0]	0.01, 0.76, 1.51, 2.25, 3.00	4.00, 4.52, 4.97, 5.39, 5.78	0.018, 0.044, −0.004, −0.057, 0.090
(0.0, 5.0]	0.01, 1.26, 2.51, 3.75, 5.00	4.00, 4.82, 5.52, 6.14, 6.71	0.018, 0.061, −0.005, −0.064, 0.101
(0.0, 10.0]	0.01, 2.51, 5.01, 7.50, 10.00	4.00, 5.52, 6.71, 7.73, 8.64	0.018, 0.086, −0.009, −0.066, 0.107

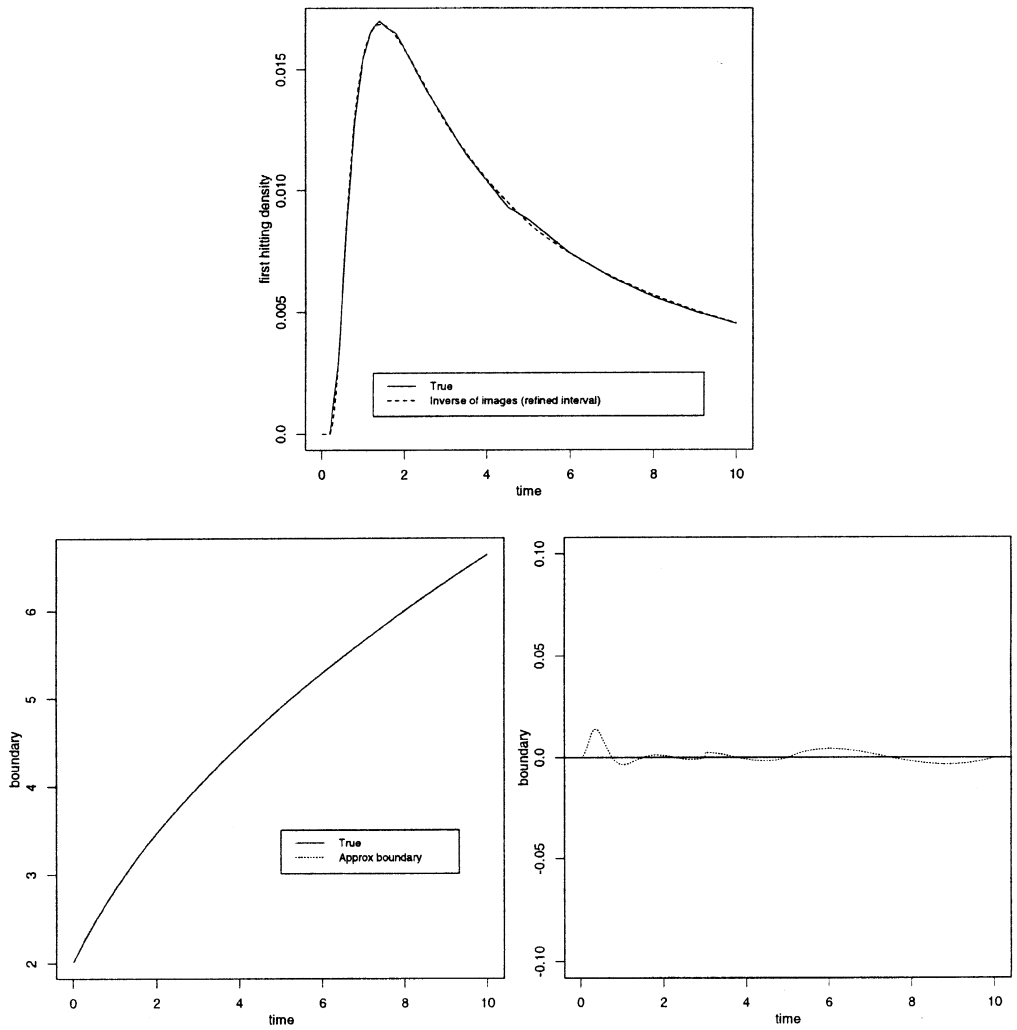

Figure 4. First hitting-time density approximation for $2\sqrt{1+t}$ (top) by the inverse method of images (refined interval). Approximate boundary (bottom left) and deviance of the approximate boundary from the true boundary (bottom right).

Here we have the boundary $0.5 - 0.5t^2$, $t > 0$, for which we obtain a first hitting-time density or distribution approximation in the time interval (0, 2] using the inverse method of images with six interpolation points (see Table 1). We shall preassign the values of the θs in the same way as in the square root boundary case using the αs from GTA1 and GTA2 for the parabolic boundary. We see from Figure 5 (top) that this density approximation is

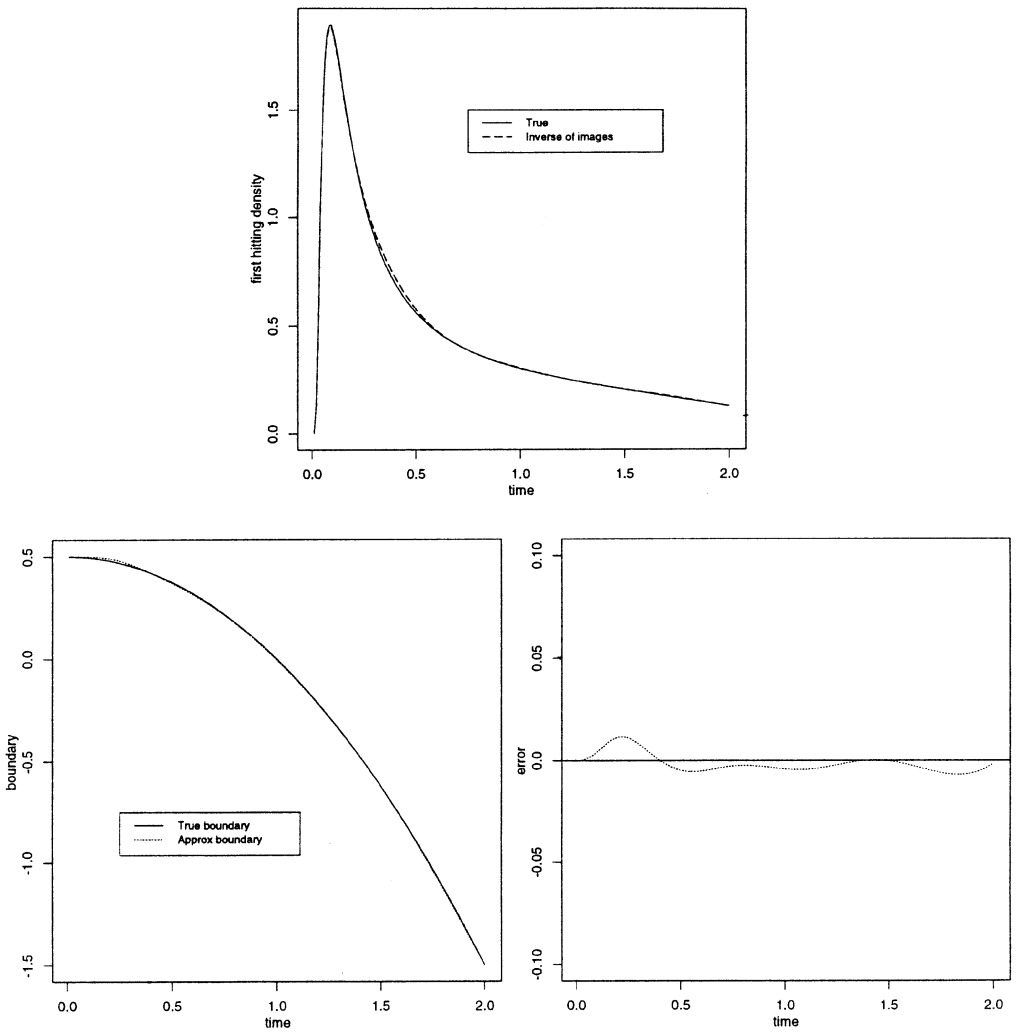

Figure 5. First hitting-time density approximation for $0.5 - 0.5t^2$ (top) by the inverse method of images. Approximate boundary (bottom left) and deviance of the approximate boundary from the true boundary (bottom right).

very close to the true density. This is reaffirmed by Figure 5 (bottom) where the associated approximate boundary is extremely close to $0.5 - 0.5t^2$ in the time interval of interest.

For the convex boundary $0.5 + 8t + 0.5t^2$, $t > 0$, in the time interval (0, 1.5], we use the inverse method of images with six interpolation points (see Table 1). We note that the approximate boundary closely interpolates the true boundary (Figure 6 (bottom)) and we

expect the associated density approximation so produced to be reasonably accurate[3] (see Figure 6 (top)). We observe here that Groeneboom (1989) expressed the first hitting-time density for convex boundaries of the form $\alpha + \beta t + \gamma t^2 (\alpha, \gamma \in \mathbb{R}_+; \beta \in \mathbb{R}; t > 0)$ in terms of integrals of Airy functions, which may require heavier numerical computations.

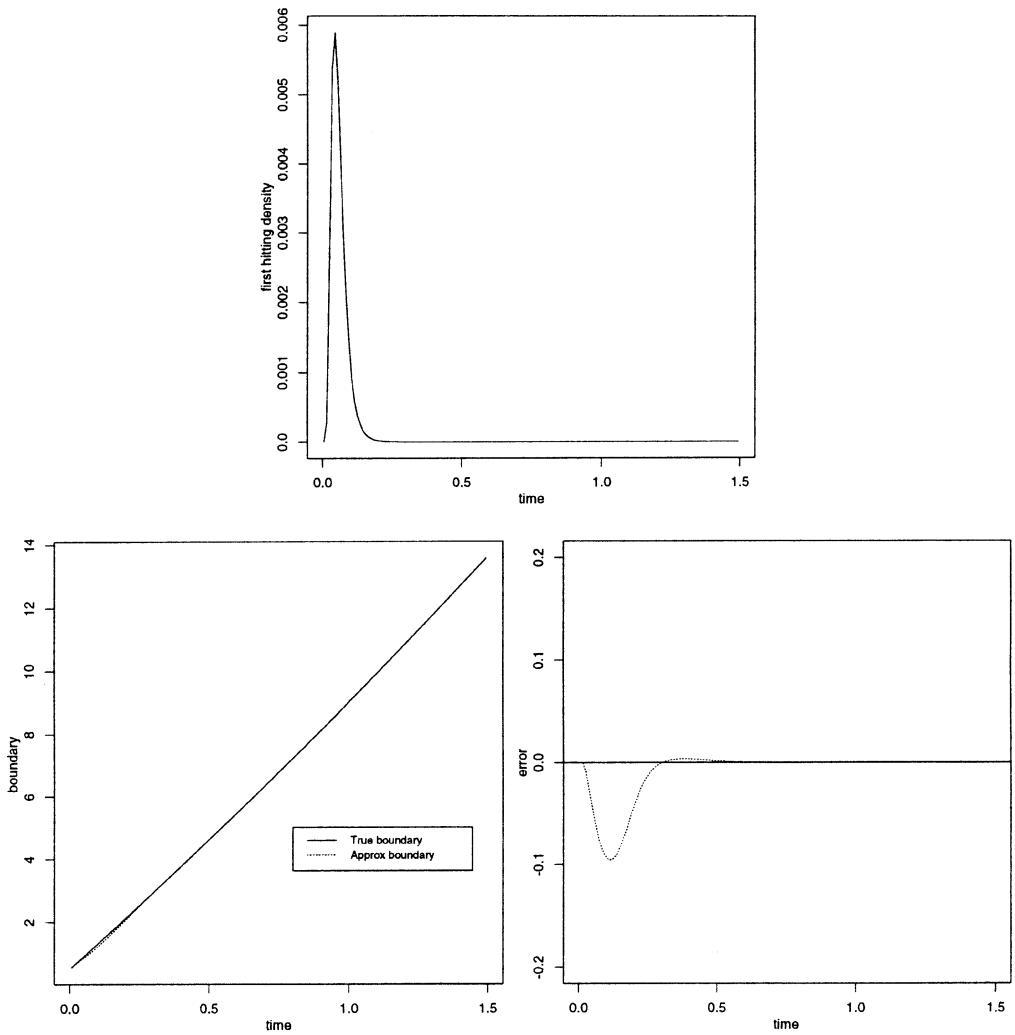

Figure 6. First hitting-time density approximation for $0.5 + 8t + 0.5t^2$ (top) by the inverse method of images. Approximate boundary (bottom left) and deviance of the approximate boundary from the true boundary (bottom right).

Table 3. Interpolations, θs and Fs used in the inverse method of images for two-sided boundaries

(ψ_+, ψ_-)	Interpolation points	θs	Fs
$(2, -2)$	0.01, 0.51, 1.01, 1.50, 2.00	4.0, 5.5, 7.0, 8.5, 10.0	$1.00, 9.65 \times 10^{-9}, -2.77 \times 10^{-3}, -7.65, 7.10 \times 10^{2}$
		$-4.0, -5.5, -7.0, -8.5, -10.0$	$1.00, 9.65 \times 10^{-9}, -2.77 \times 10^{-3}, -7.65, 7.10 \times 10^{2}$
$(2, -1)$	0.01, 0.51, 1.01, 1.50, 2.00	4.0, 4.9, 5.8, 6.6, 7.5	$1.00, 5.72 \times 10^{-4}, -3.19 \times 10^{-1}, -2.89, 9.37$
		$-2.00, -3.38, -4.75, -6.13, -7.50$	$1.00, 2.08 \times 10^{-7}, -8.48 \times 10^{-4}, -1.52, 9.14$
$(\sqrt{1+t}, -\sqrt{1+t})$	0.01, 0.51, 1.01, 1.50, 2.00	2.0, 2.5, 2.9, 3.1, 3.4	$0.37, 0.19, -0.34, 0.39, -0.11$
		$-2.0, -2.5, -2.9, -3.1, -3.4$	$0.37, 0.19, -0.34, 0.39, -0.11$
$(\sqrt{1+t}, -0.8\sqrt{1+t})$	0.01, 0.51, 1.01, 1.50, 2.00	2.0, 2.5, 2.9, 3.1, 3.4	$0.37, 0.21, -0.47, 0.66, -0.33$
		$-1.6, -2.2, -2.5, -2.8, -3.0$	$0.53, 0.23, -0.63, 0.97, -0.49$

5.2. Boundary crossing problems with two-sided boundaries

Here we consider applications of the inverse method of images to the first hitting-time density approximations for two-sided boundaries $\psi = \psi_{\pm} = (\psi_+, \psi_-) = \pm 2$, $(+2, -1)$, $\pm\sqrt{1+t}$, $(+\sqrt{1+t}, -0.8\sqrt{1+t})$ for $t > 0$.

The approximation procedures are similar to those for one-sided boundaries except that we shall add images along the negative space axes as well as the positive space axes. Our choices of the interpolation points, θs and the resulting Fs for each of the boundaries considered are given in Table 3. The first hitting-time density approximation for the upper boundary of each case, the associated approximate boundary and its deviance from the true boundary are given in Figures 7–10. By inspecting the accuracy of the corresponding approximate boundary so produced by the inverse method of images, we may check the accuracy of the first hitting-time density approximation for each case. From Corollary 4.1, the estimates are fairly accurate in these cases.

Acknowledgements

The authors would like to thank Dr. G.A. Young for implementing Dhlakama's method in Fortran. The first and second named authors would like to gratefully acknowledge the friendship, inspiration and support of the third, Henry Daniels, who sadly passed away after completion of this work, but before the paper appeared in print.

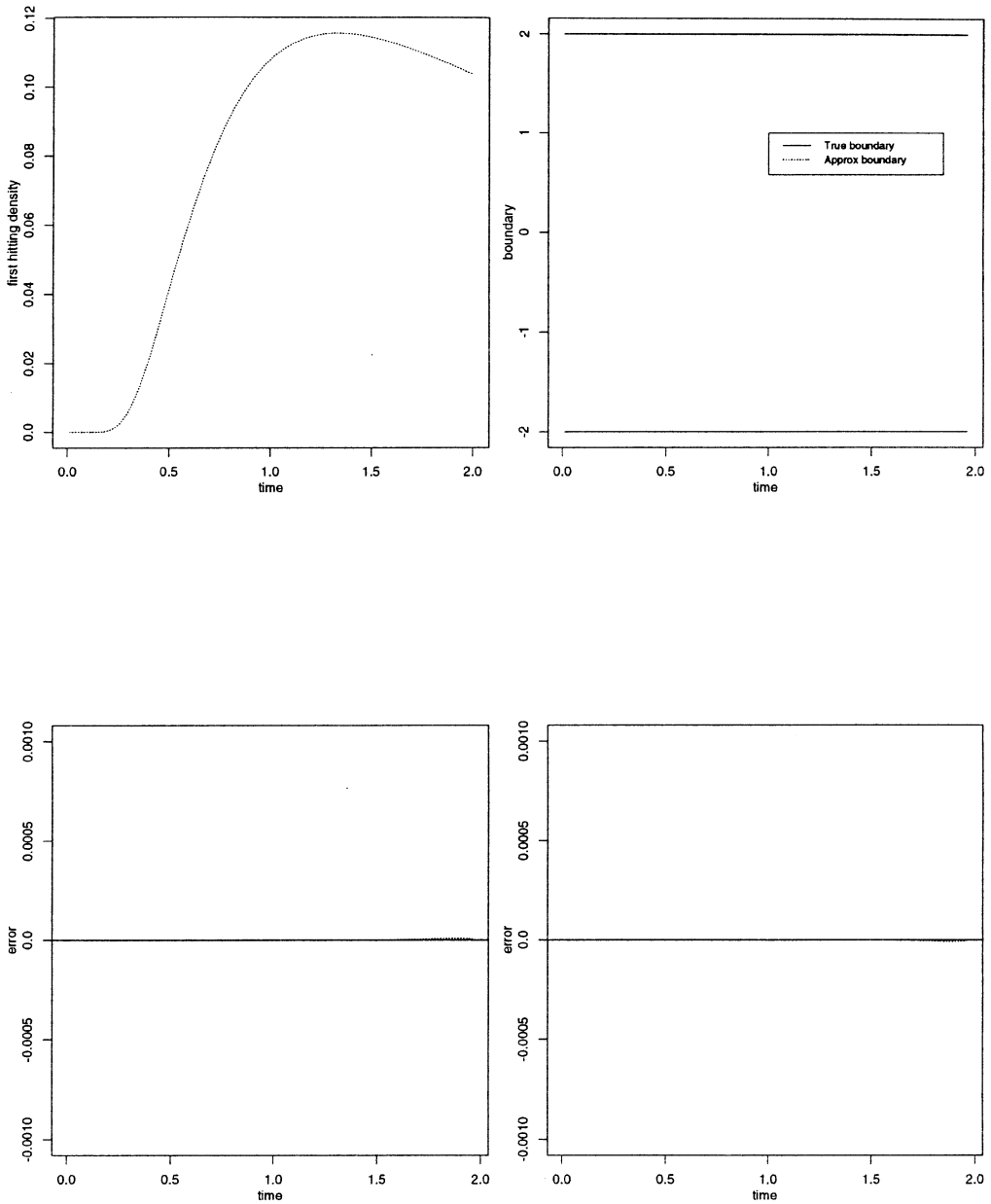

Figure 7. First hitting-time density approximation for the upper boundary of $\psi_{\pm} = \pm 2$ (top left) by the inverse method of images. Approximate boundary (top right). Deviance of the approximate upper and lower boundaries from the corresponding true boundaries (bottom left and right).

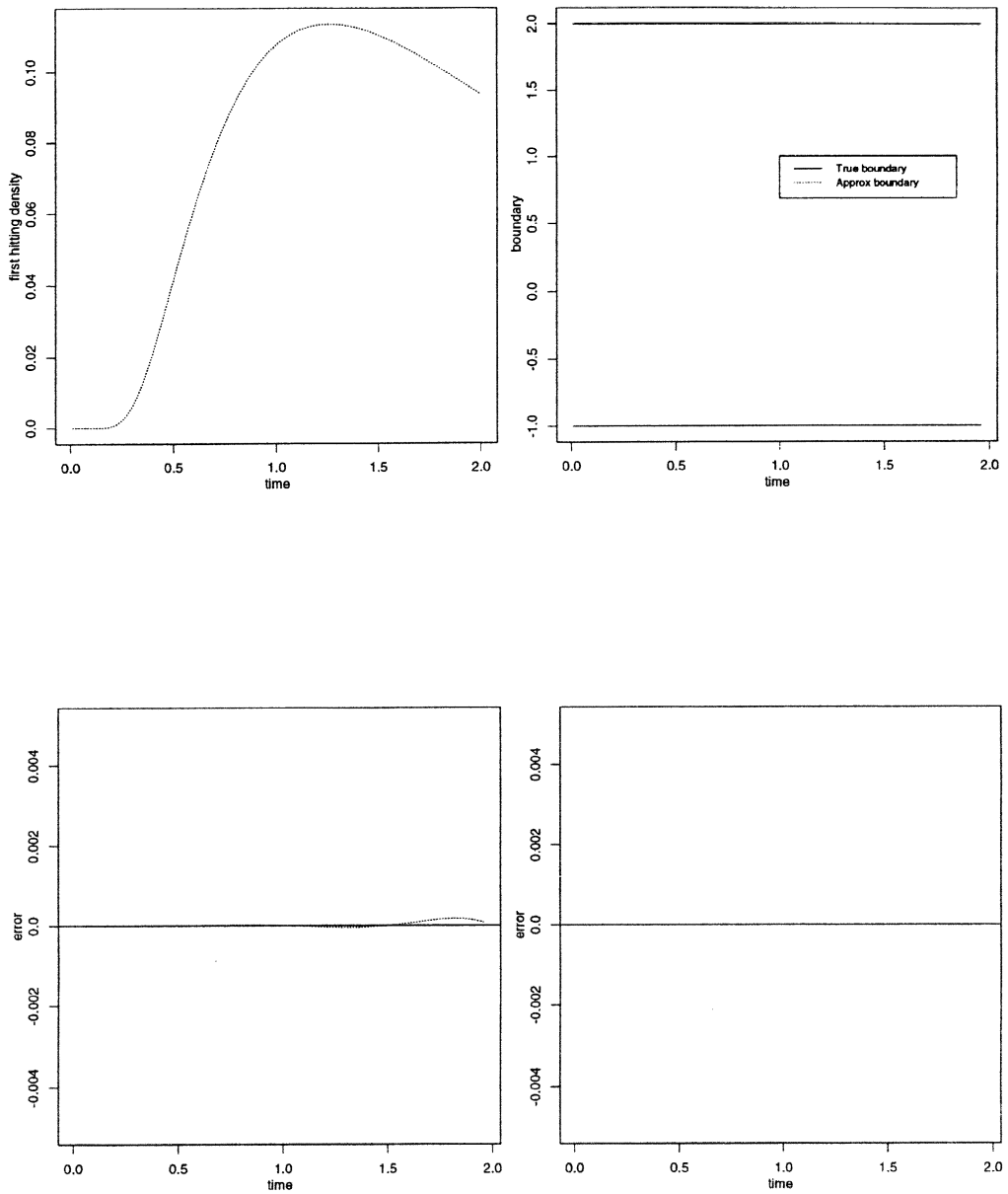

Figure 8. First hitting-time density approximation for the upper boundary of $(\psi_+, \psi_-) = (2, -1)$ (top left) by the inverse the method of images. Approximate boundary (top right). Deviance of the approximate upper and lower boundaries from the corresponding true boundaries (bottom left and right).

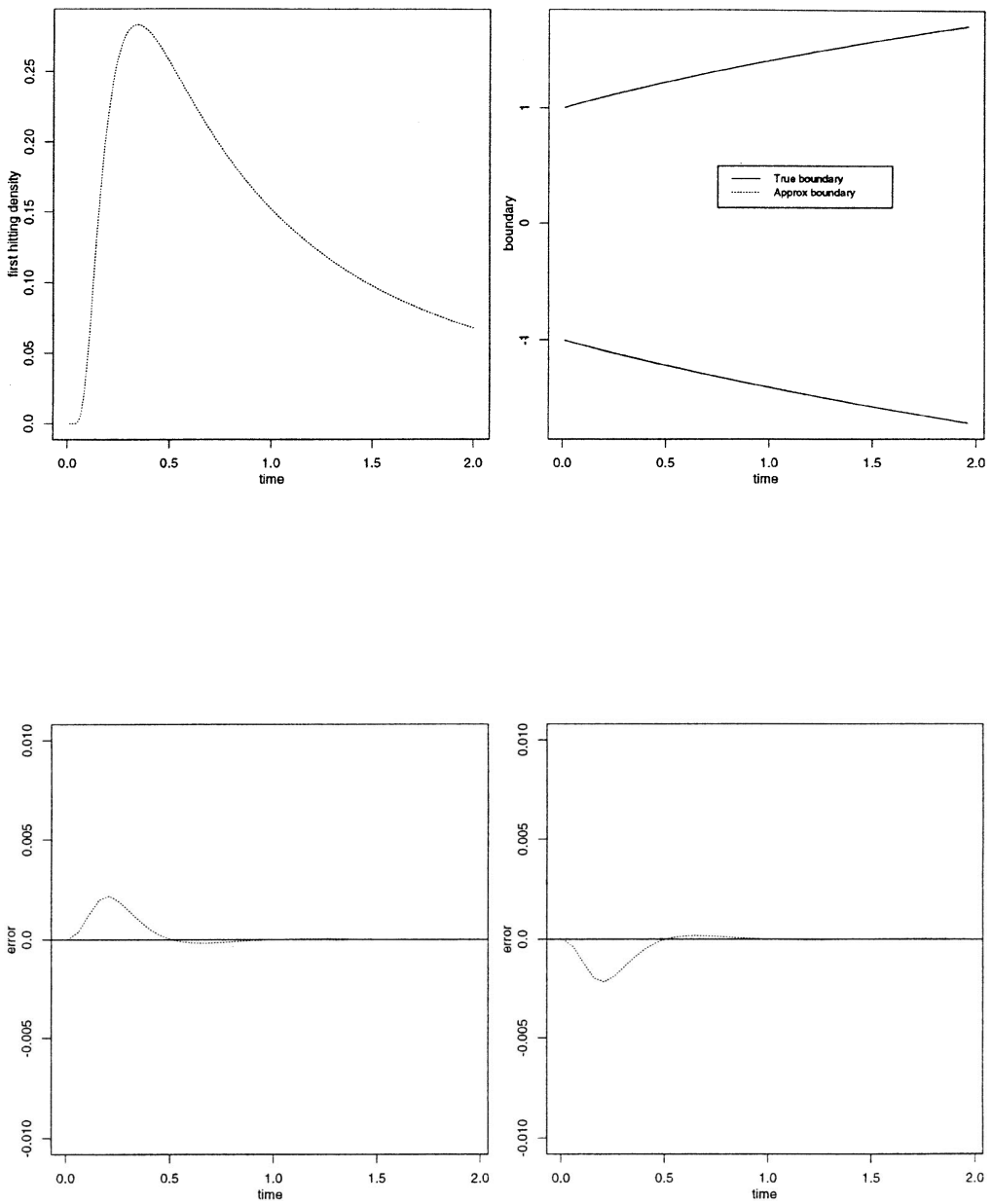

Figure 9. First hitting-time density approximation for the upper boundary of $\psi_{\pm} = \pm\sqrt{1+t}$ (top left) by the inverse method of images. Approximate boundary (top right). Deviance of the approximate upper and lower boundaries from the corresponding true boundaries (bottom left and right).

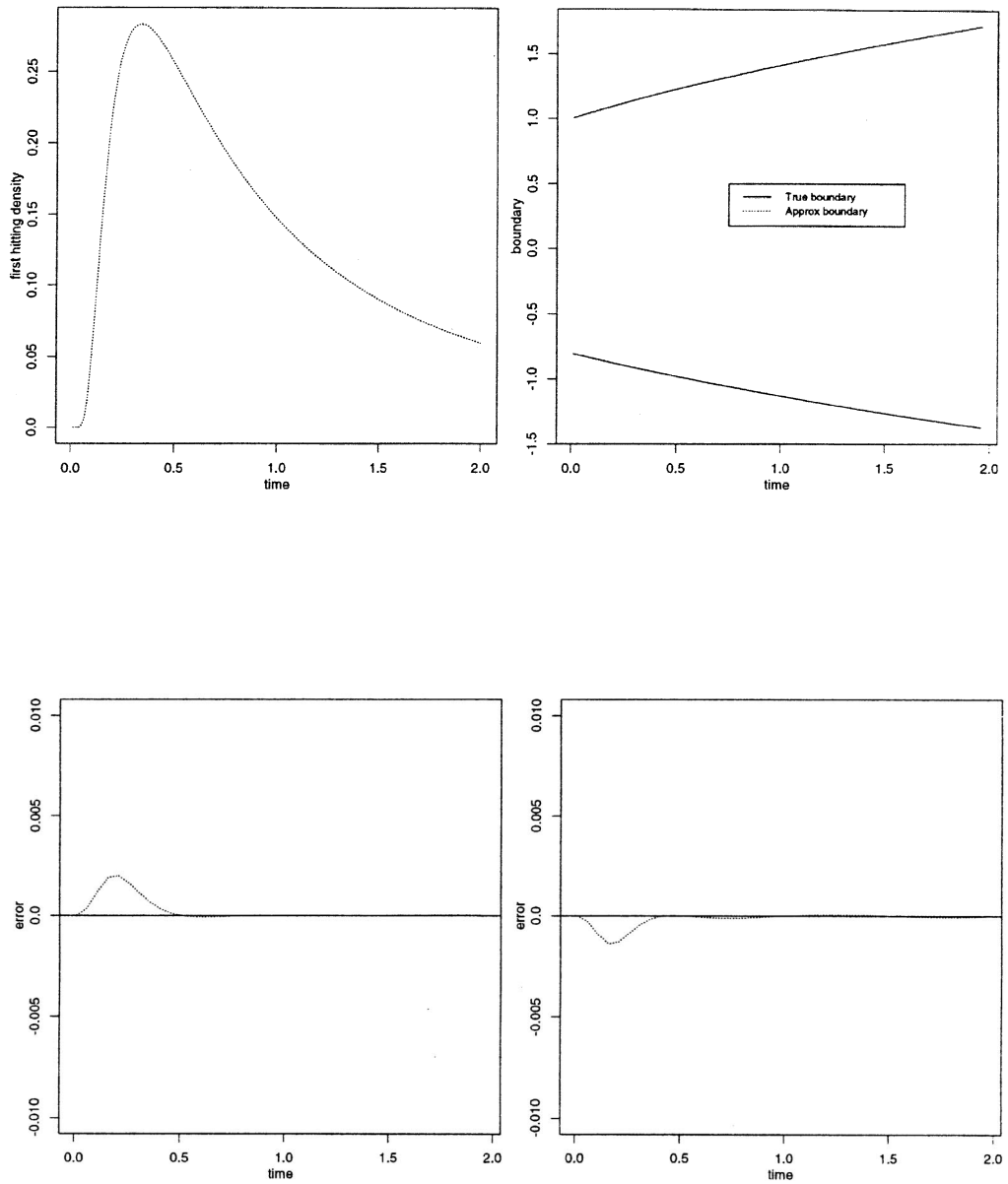

Figure 10. First hitting-time density approximation for the upper boundary of $(\psi_+, \psi_-) = (\sqrt{1+t}, -0.8\sqrt{1+t})$ (top left) by the inverse method of images. Approximate boundary (top right). Deviance of the approximate upper and lower boundaries from the corresponding true boundaries (bottom left and right).

References

Daniels, H.E. (1969) The minimum of a stationary Markov process superimposed on a U-shaped trend. *J. Appl. Probab.*, **6**, 399–408.

Daniels, H.E. (1982) Sequential tests constructed from images. *Ann. Statist.*, **10**, 394–400.

Daniels, H.E. (1996) Approximating the first crossing-time density for a curved boundary. *Bernoulli*, **2**, 133–143.

Dhlakama, R. (1994) Numerical approximation of an epidemic density function. Research report, Institute of Acturial Mathematics and Mathematical Statistics, Stockholm University.

Durbin, J. (1992) The first-passage density of the Brownian motion process to a curved boundary (with appendix by D. Williams). *J. Appl. Probab.*, **29**, 291–304.

Groeneboom, P. (1989) Brownian motion with a parabolic drift and Airy functions. *Probab. Theory Related Fields*, **81**, 79–109.

Keilson, J. and Ross, H.F. (1975) Passage time distributions for Gauss Markov (Ornstein–Uhlenbeck) statistical processes. In *Selected Tables in Mathematical Statistics*, Vol. 3, pp. 233–327. Providence, RI: American Mathematical Society.

Lerche, H.R. (1986) *Boundary Crossing of Brownian Motion*, Lecture Notes in Statist. 40. Berlin: Springer-Verlag.

Lo, S.F. (1997) Boundary hitting time distributions of one-dimensional diffusion processes. Ph.D. thesis, Statistical Laboratory, University of Cambridge.

Roberts, G.O. (1991) A comparison theorem for conditional Markov processes. *J. Appl. Probab.*, **28**, 74–83.

Roberts, G.O. and Shortland, C.F. (1995) The hazard rate tangent approximation for boundary hitting times. *Ann. Appl. Probab.*, **5**, 446–460.

Strassen, V. (1967) Almost sure behaviour of sums of independent random variables and martingales. In L. LeCam and J. Neyman (eds), *Proceedings of the Fifth Berkeley Symposium on Mathematical Statistics and Probability*, Vol. II, Part 1, pp. 315–343. Berkeley: University of California Press.

Received July 1999 and revised January 2001